Modeling and Control of a Multi-Mode Heat Pump

Bortoff, Scott A.; Qiao, Hongtao; Laughman, Christopher R.

TR2024-111   August 22, 2024

Abstract

Modern heat pumps have evolved significantly in the last 50 years to provide energy efficient cooling and heating in a broad range of conditions. However, one consequence of improved building codes and higher energy efficiency standards is that heat pumps can struggle to maintain comfortable levels of indoor humidity in some conditions and applications, especially in humid climates. This paper considers modeling and control of a residential heat pump system that can operate in several modes, including a conventional cooling mode and a reheat mode. In the reheat mode, condensed (warm) refrigerant is passed through an indoor heat exchanger to reheat the conditioned air. The configuration and action of feedback reduces the evaporator temperature, resulting in an increased rate of water condensation and reduced indoor relative humidity level. A control algorithm is proposed that coordinates the actions of the variable speed compressor, electronically actuated expansion valves and variable speed fans to achieve both indoor air temperature regulation and indoor humidity regulation. The algorithm includes hybrid logic to switch among operating modes. Simulations of the multi-mode heat pump coupled coupled with a dynamic model of a typical residential building located in a humid climate zone demonstrate both temperature and humidity regulation.

IEEE Conference on Control Technology and Applications (CCTA) 2024

Modeling and Control of a Multi-Mode Heat Pump

Scott A. Bortoff, Hongtao Qiao and Christopher R. Laughman[1]

Abstract— Modern heat pumps have evolved significantly in the last 50 years to provide energy efficient cooling and heating in a broad range of conditions. However, one consequence of improved building codes and higher energy efficiency standards is that heat pumps can struggle to maintain comfortable levels of indoor humidity in some conditions and applications, especially in humid climates. This paper considers modeling and control of a residential heat pump system that can operate in several modes, including a conventional cooling mode and a reheat mode. In the reheat mode, condensed (warm) refrigerant is passed through an indoor heat exchanger to reheat the conditioned air. The configuration and action of feedback reduces the evaporator temperature, resulting in an increased rate of water condensation and reduced indoor relative humidity level. A control algorithm is proposed that coordinates the actions of the variable speed compressor, electronically actuated expansion valves and variable speed fans to achieve both indoor air temperature regulation and indoor humidity regulation. The algorithm includes hybrid logic to switch among operating modes. Simulations of the multi-mode heat pump coupled coupled with a dynamic model of a typical residential building located in a humid climate zone demonstrate both temperature and humidity regulation.

I. Introduction

Heat pumps are the only viable technology for scalable electrification of residential building heating, ventilation and air conditioning (HVAC). A heat pump provides indoor heating or cooling using a closed vapor compression cycle to move heat from a lower temperature fluid to a higher temperature fluid. When operating in cooling mode, a heat pump removes both sensible heat (reducing temperature) and latent heat through condensation (reducing absolute humidity) from the indoor air. For at least 50 years, increasingly stringent energy efficiency standards have resulted in heat pump products with improved energy efficiency and performance [1], largely by the introduction of variable speed compressors and fans, and electronically actuated expansion valves (EEVs), which allow modern heat pumps to operate efficiently over a wide range of operating conditions, if properly controlled. From the control scientist's point of view, modern heat pumps are multivariable, interactive, hybrid (operate in multiple modes) and nonlinear, demanding a rigorous application of model-based control design [2], [3], [4].

Despite its evolution, a modern heat pump may provide poor latent heat performance in some conditions and applications, resulting in unacceptably high levels of indoor relative humidity [5]. This can occur for three reasons. First, some heat pump manufacturers have modified their products over the years to improve their energy efficiency ratings,

by changing heat exchanger coil geometry for example [6]. This raises the evaporating temperature and improves energy efficiency, but reduces the latent heat capacity. Second, building codes have evolved to call for higher amounts of insulation and tighter construction, in order to reduce outdoor air infiltration. This results in lower sensible heat loads on HVAC equipment. But even tight construction can allow for 0.25 outdoor air changes per hour (ACH) by infiltration [7]. In humid climates, where outdoor relative humidity can be 100% overnight, infiltration can drive indoor humidity above comfortable levels [5]. Third, HVAC equipment is often oversized for the application, resulting in on-off cycling that results in elevated indoor relative humidity levels [8].

Fig. 1 shows the result of a simulation that illustrates this behavior. The system includes a heat pump operating in cooling mode in which the indoor unit is of the forced-air type commonly used in North America (NA). The heat pump was modeled in the Modelica language (described in more detail in Section III) and was coupled to a model of a house constructed to meet modern building codes for Houston TX, US (representing a very humid climate zone) and used typical meteorological year (TMY) weather data for Houston [9], [10]. The simulation began at midnight following a hot summer day, and ran for 27h, including overnight, the following (hot) day, and a second night. Initially the building constructions and indoor air were $30°C$ and 40% relative humidity. The heat pump pulled down the air temperature to the $22°C$ set point within an hour. Soon after, the compressor speed, driven by feedback, dropped to its minimum speed limit, and then the system cycled on and off for the remainder of the night because of the low sensible heat load. As a result, the latent heat capacity of the indoor heat exchanger was relatively low, and the indoor relative humidity increased overnight, until it reached 80%. Once the sun rose the next day, the compressor speed increased due to the increased sensible heat load, again as the result of feedback, and the relative humidity dropped, but it peaked above 80% the second night. Although this particular simulation represents an extreme condition, high indoor relative humidity in humid climate zones, especially overnight, is a very real problem. We note that heat pump cycling, and in particular the behavior when both the compressor and fans are stopped and restarted, is captured, enabled by our use of Modelica [11], [12], [13].

In this paper we consider the multi-mode heat pump diagrammed in Fig. 2, which incorporates a reheat coil in the indoor air handler. This system runs in either a conventional cooling mode, in which the indoor reheat coil is bypassed, or a reheat mode, in which the reheat coil receives

[1] Authors are with Mitsubishi Electric Research Laboratories, Cambridge, MA, USA {`bortoff, qiao, laughman`}@merl.com
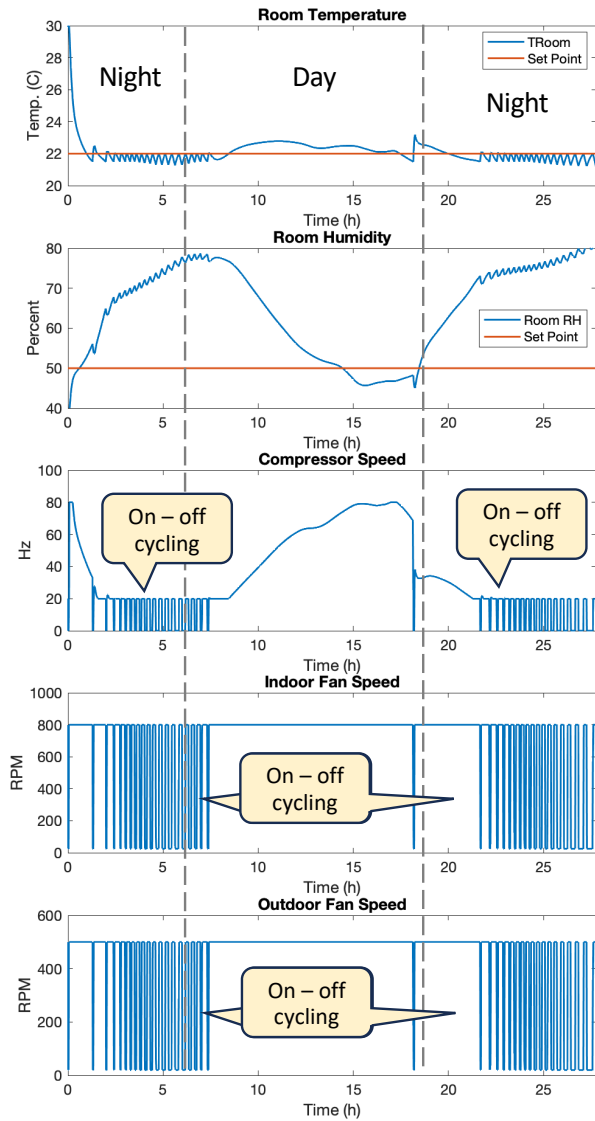
Fig. 1. Heat pump simulation, showing cooling mode operation overnight in humid climate, with zone temperature (top), zone humidity (second), compressor speed (third) and indoor and outdoor fan speeds (bottom two).

Fig. 2. Multi-mode heat pump system.

condensed, warm refrigerant from the outdoor coil, which adds sensible heat to the conditioned airstream. This affects the thermodynamics to reduce the evaporator temperature, which condenses more water, resulting in a reduction in indoor relative humidity.

We propose a controller for this system that includes compensated feedback loops for the compressor, the two EEVs and both the indoor and outdoor fan speeds, designed to regulate both the indoor air temperature and the indoor relative humidity to set points. In addition, logic for switching among cooling, reheat and off modes of operation is defined. The coordinated control algorithm of the indoor and outdoor fan speeds in reheat mode, together with the mode switching logic, are the primary contributions of this paper.

Simultaneous control of temperature and humidity using compressor and indoor fan speeds for a conventional heat
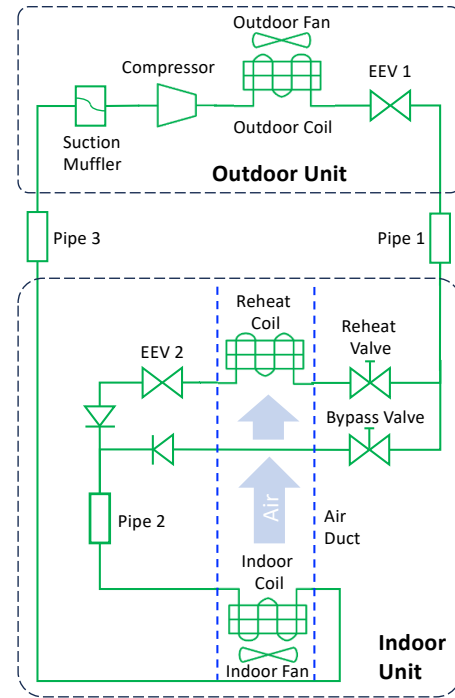
pump was first addressed using physics-based models and experiment in [14], later analyzed in [15], and is by now well known and widely practiced in industry. Our results are similar in nature but use more modern modeling technology (Modelica) and methods of robust multivariable control, introduce the reheating coil, and include hybrid switching logic. Related results include an on-off control algorithm for simultaneous temperature and humidity control [16]. Condenser reheat intended for simultaneous temperature and humidity control is also well known and widely practiced [17], [18] but results for robust feedback to automate operation is lacking in the literature. The relatively recent [6] surveys temperature and humidity control equipment and control methodologies.

This paper is organized as follows. In Section II, we describe the proposed system in more detail, and system-level dynamic models of the system and building are described in Section III. In Section IV we describe the control strategy and its realization in the Modelica modeling language. Simulation results are presented in Section V, showing regulation of both room temperature and relative humidity, and also the mode switching behavior. Some conclusions on the subjects of heat pumps, object oriented modeling are offered in Section VI.

II. SYSTEM DESCRIPTION

The multi-mode heat pump diagrammed in Fig. 2 consists of a conventional outdoor unit connected by pipes to a modified indoor air handler unit. The outdoor unit consists of a variable speed compressor, which includes a suction muffler, an outdoor coil, which is a condensing tube-fin heat

TABLE I

CONTROL INPUTS, MEASURED OUTPUTS & DISTURBANCES.

Name	Description
OFS	Outdoor fan speed (RPM)
IFS	Indoor fan speed (RPM)
CF	Compressor frequency (Hz)
EEV 1	Outdoor electronic expansion valve (counts)
EEV 2	Indoor electronic expansion valve (counts)
Reheat	Reheat valve (boolean)
Bypass	Bypass valve (boolean)
T_r	Measured indoor air temperature (°C)
ϕ_r	Measured indoor air relative humidity (%)
T_a	Measured outdoor air temperature (°C)
T_d	Measured compressor discharge temperature (°C)
T_e	Measured evaporator temperature (°C)
T_s	Measured suction port temperature (°C)
Q_s	Sensible indoor heat load disturbance (W)
Q_l	Latent indoor heat load disturbance (W)

Fig. 3. Operating envelope in disturbance space for a range of CF, IFS & OFS with cooling mode (right) and reheat mode (left), at $T_r = 22°C$ and $\phi_r = 50\%$. The two regions lack overlap for clarity. In practice, the reheat coil is sized (smaller) to ensure overlap so that no load combination lies outside a controllable region.

exchanger (HEX) with a variable speed fan, and electronic expansion valve EEV 1. The indoor air handler unit includes an indoor coil, which is an evaporating tube-fin HEX with a variable speed fan, commonly called an A-coil because of its shape, the reheat coil, located downstream (air-wise) of the A-coil, and a pair of on/off valves to change its mode of operation. In conventional cooling mode, the bypass valve is opened, the reheat valve closed, and the reheat coil is not included in the cycle. In reheat mode, the reheat valve is opened, the bypass valve is closed, and the reheat coil is included in the cycle.

The cycle operates as follows. Refrigerant vapor is compressed by the compressor, raising its pressure and temperature. It flows into the outdoor coil, where it fully condenses into liquid, releasing heat to the outdoor air. In cooling mode, the outdoor expansion valve, EEV 1, is used as the expansion device. As the refrigerant passes through EEV 1, its pressure and temperature drop and it becomes cold, two-phase fluid, which passes through pipe 1, the bypass valve, pipe 2 and into the A-coil, where it entirely evaporates, absorbing heat from the indoor air stream. The low pressure vapor is returned to the compressor via pipe 3, closing the cycle.

In reheat mode, the outdoor EEV 1 is opened to its maximum value, so that the its pressure (and temperature) drop is minimized. After partial expansion, the still warm refrigerant passes through pipe 1, the reheat valve and into the reheat coil, where it heats the conditioned indoor air stream. It then passes through expansion valve EEV 2, which is used as the primary expansion device. As the refrigerant passes through EEV 2, its pressure and temperature drop and it becomes cold two-phase fluid, which passes through pipe 2 and into the A-coil, where it entirely evaporates, absorbing heat from the indoor air stream. The low pressure vapor is returned to the compressor via pipe 3, closing the cycle. Several check valves prevent undesired refrigerant back flow, and a set of additional pipes and valves, not shown, allow the flow of refrigerant to be reversed for heating mode, which is beyond the scope of the paper.

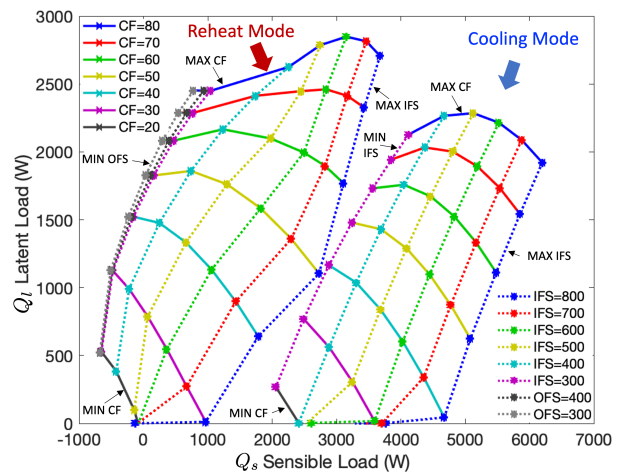The purpose of reheat mode is to provide an increased

latent heat capacity relative to cooling mode, in order to remove excess humidity from the indoor air. This is achieved in two ways. First, when the reheat mode is operational, the refrigerant in the reheat coil is cooled by the airstream coming off the A-coil, which is approximately $10 - 15°C$ and usually colder than the outdoor air. This results in a colder liquid refrigerant entering EEV 2, and therefore colder two-phase refrigerant entering the A-coil, which therefore condenses more water. Second, because the reheat coil adds sensible heat to the conditioned air, the feedback controller (described in Section IV) increases the compressor speed as the result of integral action, in order to regulate the indoor air temperature to its set point. As a result, the A-coil cools and condenses more water. Both of these effects combine to reduce the temperature of the A-coil, and therefore increase the amount of latent heat removed from the indoor air.

Fig. 3 diagrams the operating envelope in both cooling and reheat modes for a particular heat pump in the disturbance space (Q_s, Q_l). In each region, there exist values of CF, IFS and OFS to reject constant values of Q_s and Q_l with zero steady-state error, for $T_r = 22°C$ and $\phi_r = 50\%$. This plot shows the limitations of cooling-only mode (the right region), which does not cover low levels of Q_s, and also the region for which reheat mode is useful.

III. SYSTEM MODELING

Several dynamic models of the multi-mode heat pump coupled to various building models were constructed in the Modelica modeling language [12], [19] for purposes of developing control algorithms and evaluating closed-loop system performance in representative buildings and climates. Modelica has three features that make it unique and indispensable for model-based design of such a complex multi-physical system.

1) It is a declarative, acausal, equation-based language with a hybrid differential algebraic model of compu-

tation. Equations representing heat transfer, fluid mechanics, thermodynamics and control are transcribed through declarations and mathematical statements. In particular, causality among variables need not be presumed by the modeler (as is the case with a signal-flow language such as Matlab Simulink) but rather is computed by the modeling tool during a simulation. This means that the direction of fluid flow in the components and the cycle is not assumed a priori by the modeler, but is computed by the model at simulation time. Fluid flow direction can change dynamically during a simulation, or go to zero. For example, fluid direction can change when the compressor is turned off, when a fan is turned off, or when valves are opened or closed to change operating mode. A *single* hybrid model of the cycle was therefore constructed that represents the complete, hybrid thermofluid behavior, so that the system could be simulated as it transitioned among cooling, reheat and off states.

2) Modelica is component-oriented, with object-oriented features for organization. This makes it possible to organize models and model libraries and reuse code.

3) Modelica is open-source with an active and enthusiastic user community. Commercial and open-source libraries, such as the Buildings library [9], represent dozens of person-years of modeling effort.

The dynamic models were organized by components, with a set of declared differential and algebraic equations for each component. The components were connected together to equate potential, flow and stream variables at each component boundary, resulting in a large set of nonlinear differential-algebraic equations. The Dymola tool then compiled these equations into a form suitable for time-domain simulation.

The variable-speed compressor was modeled with a set of coupled, nonlinear algebraic equations that relate the compressor speed, refrigerant mass flow rate, inlet and outlet pressures, enthalpies and densities, respectively, to one another. The electric expansion valves were modeled conventionally as $\dot{m} = C_v\sqrt{\rho_{in}\Delta p}$, where $\dot{m}$ is the refrigerant mass flow rate, ρ_{in} is the refrigerant inlet density, Δp is the pressure drop across the valve, and C_v depends on the valve opening command and was fit to laboratory data.

Three-dimensional, finite volume models of heat and fluid flow were used for the HEXs. Each was divided into a number of segments, one per tube, and each segment was divided into three sections: The refrigerant stream, the finned walls, and the air stream. The refrigerant stream was described by a one-dimensional flow with fluid properties varying only in the direction of flow. Conservation of mass, momentum and energy for each segment was modeled as [20], [21]

$$\frac{\partial(\rho A)}{\partial t} + \frac{\partial(\rho A v)}{\partial x} = 0 \tag{1}$$

$$\frac{\partial(\rho v A)}{\partial t} + \frac{\partial(\rho v^2 A)}{\partial x} = -A\frac{\partial P}{\partial x} - F_f \tag{2}$$

$$\frac{\partial(\rho u A)}{\partial t} + \frac{\partial(\rho v h A)}{\partial x} = vA\frac{\partial P}{\partial x} + vF_f + \frac{\partial Q}{\partial x}, \tag{3}$$

where ρ is the density, A is the cross-sectional area of the flow, v is the velocity, P is the pressure, F_f is the frictional pressure drop, u is the specific internal energy, h is the specific enthalpy, and Q is the heat flow rate into or out of the fluid. For the air stream, the energy balance equation

$$\dot{m}_a c_{p,a}\frac{dT_a}{dy}\Delta y = \alpha_a\left(A_{0,t} + \eta_{\text{fin}}A_{0,\text{fin}}\right)\left(T_w - T_a\right) \tag{4}$$

was used, where $\dot{m}_a$ is the airflow, T_a is the air temperature, T_w is the wall temperature, $c_{p,q}$ is a heat capacity. Finally, the energy balance equation for tube and fin heat conduction was

$$\left(M_t c_{p,t} + M_{\text{fin}}c_{p,\text{fin}}\right)\frac{dT_w}{dt} = q_r + q_a \tag{5}$$

$$q_r = \alpha_r A\left(T_r - T_w\right) \tag{6}$$

$$q_a = \dot{m}_a\left(c_{p,q}(T_{a,\text{in}} - T_{a,\text{out}})\right), \tag{7}$$

where M_t is the tube wall mass, M_{fin} is the fin mass, q_r is the heat flux from the refrigerant, q_a is the heat flux to the air, T_w is the tube wall temperature, $T_{a,\text{in}}$ is the inlet air temperature, and $T_{a,\text{out}}$ is the outlet air temperature. This model allows for complex tube circuiting and also for split refrigerant flow. The balance equations were augmented with a set of empirical closure relations describing the single- and two-phase heat transfer coefficients and frictional pressure drops for the fluid on both the refrigerant and air sides. These equations were discretized using the Reynolds transport theorem using a staggered-grid approach along their respective flow directions, and transcribed into Modelica.

The heat pump system model was coupled to both an adiabatic single-volume room model for understanding the basic dynamics, and a two-zone building model representing a typical residential construction in Houston TX, USA [10], based on the Modelica Buildings Library [9], for more realistic performance evaluation. This model captures convective, conductive and radiative heat transfer to and from the environment, along with air transport within the building, air infiltration from outside, and TMY weather.

IV. CONTROL STRATEGY

The proposed control algorithm is comprised of three parts: 1) A conventional inner loop controls the compressor frequency CF and the expansion devices EEV 1 and EEV 2; 2) A novel outer loop controls the indoor fan speed IFS and outdoor fan speed OFS; and 3) boolean logic for switching among cooling, reheat and off modes. The objective is to regulate both the indoor temperature T_r and relative humidity ϕ_r to set-points $\bar{T}_r$ and $\bar{\phi}_r$, respectively, with zero steady-state error for constant values of heat load disturbances, if possible. (Because all actuators have limits and the heat pump is limited in its capacity, some set-points may not be feasible.) Closed-loop stability with some robustness margin is obviously required. Further, both set points must be reached *simultaneously*. This adjective is used frequently in the literature to mean that both T_r and ϕ_r are regulated
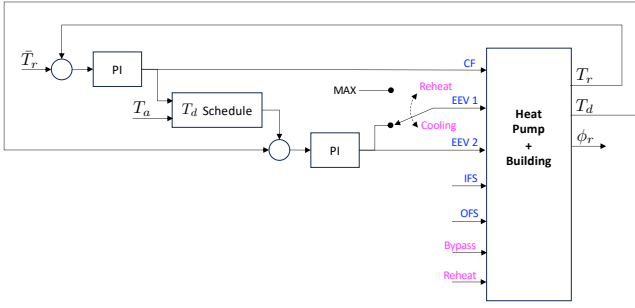
Fig. 4. Inner feedback loop showing continuous control variables in blue and boolean control variables in magenta. PI blocks denote proportional-integral compensators with anti-windup, and the T_d schedule is a function taking CF and T_a as input and computing a reference value for T_d.
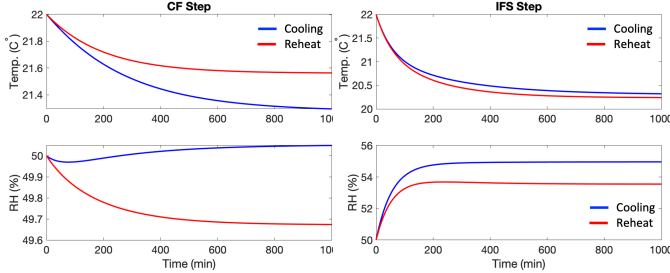

Fig. 5. Open loop step responses in cooling and reheat modes, at $22°$C and 50% RH. Note the non-minimum phase response from CF to RH in cooling mode.

Fig. 6. $\Delta T - \Delta \phi$ chart showing the control directions at an equilibrium condition indicated by the green dot, in cooling mode (blue) and reheat mode (red), and contours for wet bulb temperature and ρ (gray), respectively. The set-point is $22°$C and $\phi = 50\%$.

in a multivariable sense. Herein "simultaneous" means more than that. It means that the two set points are achieved at the same point in time, and in particular an overcooled condition in which $T_r < \bar{T}_r$ and $\phi_r > \bar{\phi}_r$ must be avoided because the equipment will shut off without reducing the indoor humidity to its set point.

The inner loop diagrammed in Fig. 4 is conventional [22]. The two feedback loops drive T_r to its set point $\bar{T}_r$ and the compressor discharge temperature T_d to a scheduled reference value, which indirectly regulates the evaporator super-heat $T_s - T_e$ to a small positive value. Additional selector logic is used to enforce process variable constraints but is omitted for simplicity. In cooling mode, the outdoor EEV 1 is used (and EEV 2 is not part of the refrigerant cycle), while in reheat mode, EEV 1 is set to its maximum value and EEV 2 is used to close the loop.

In both modes, an outer feedback loop is used to drive ϕ_r to a the set point $\bar{\phi}_r$ using IFS and OFS, and is derived by referring to Figs. 5 and 6. The Modelica model described in Section III was linearized about a set of steady-state operating points, and reduced-order models were computed from IFS, OFS and CF to T_r and ϕ_r. Fig. 5 shows a typical step response from CF and IFS to T_r and ϕ_r, in both cooling and reheat modes. The function from CF to T_r is approximately first order, as is the function from IFS to ϕ_r, as expected. However, in cooling mode, the function from CF to ϕ_r is in fact non-minimum phase, with a negative steady-state gain. This is a consequence of the low latent heat capacity of the system and psychometrics: As air is cooled, it can
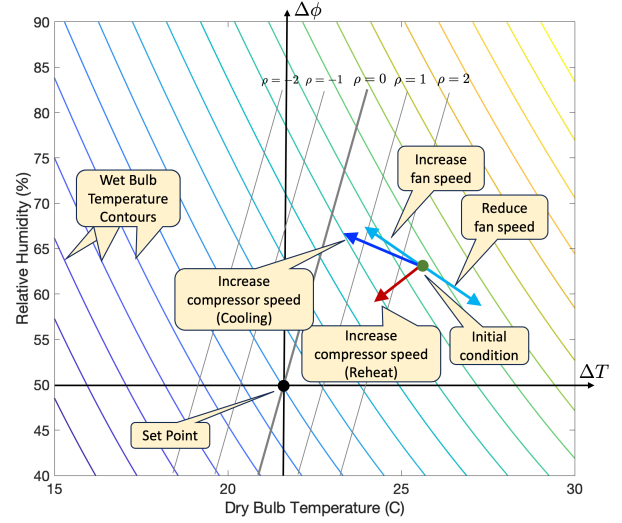
hold less water vapor, so the relative humidity can actually increase even though the absolute humidity is reduced. In the short time scale, ϕ_r is initially reduced by the colder coil condensing more water, but as the room temperature is more slowly reduced, ϕ_r increases. Therefore, CF (and LEV) is paired to regulate T_r (and T_d), as in Fig. 4, while IFS is used to regulate ϕ_r in cooling mode. The relative gain array (RGA) for the plant (CF, IFS, LEV) $\rightarrow (T_r, \phi_r, T_d)$ in cooling mode for a typical operating condition is

$$
\text{RGA} = \begin{bmatrix} 1.23 & 0.12 & -0.35 \\ -0.03 & 0.90 & 0.13 \\ -0.20 & -0.01 & 1.21 \end{bmatrix} \tag{8}
$$

makes clear the correct pairing and the small amount of two-way interaction we should expect [23]. Swapping these is poor control engineering practice, as observed in [14]. (Note that OFS is not effective in regulating either T_r or ϕ_r in cooling mode, and is controlled for other purposes.)

In reheat mode, however, both IFS and OFS are effective controls used to regulate ϕ_r. OFS becomes particularly effective when IFS is low, meaning the gain from OFS to ϕ_r is sufficient for closed loop control in this condition. Fig. 6 is a plot of T_r vs. ϕ_r, with the origin being the set point $(\bar{T}_r, \bar{\phi}_r)$, and axes $\Delta T = T_r - \bar{T}_r$ and $\Delta \phi = \phi_r - \bar{\phi}_r$. Steady-state gains computed from the family of linearizations may be visualized for both cooling and reheat modes. In cooling mode, the direction from CF, indicated by the blue arrow, shows that an increase in CF from the equilibrium condition indicated by the green dot will cause a decrease in ΔT and an increase in $\Delta \phi$. This is precisely the behavior described in the Section I and above. The red arrow indicates the control direction from CF in reheat mode, and the directions of both fan speeds IFS and OFS in reheat mode are shown in cyan. In reheat mode, an increase in CF causes a decrease in both ΔT and $\Delta \phi$, driving the system toward the origin, while
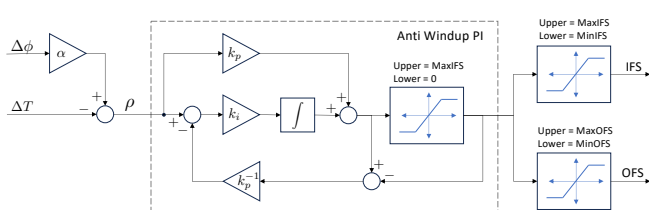
Fig. 7. Block diagram of the fan speed controller.

Fig. 8. $\Delta T - \Delta \phi$ chart showing the operating modes. The set-point is $22°$C and $\phi = 50\%$.

an increase in either IFS or OFS, which overlap, causes a decrease in ΔT but an increase in $\Delta \phi$.

This elementary observation suggests both a strategy to control both fan speeds in reheat mode, and also a strategy for defining logic to switch between cooling and reheat modes. First, we define a coordinate transformation to better align the control directions with the variables being controlled. Let

$$\rho = \alpha \Delta \phi - \Delta T, \qquad (9)$$

where $\alpha > 0$, and consider the coordinates $(\Delta T_{wb}, \rho)$, where $\Delta T_{wb} = T_{wb} - \bar{T}_{wb}$, and T_{wb} is the indoor wet bulb temperature, which is a function of T_r and ϕ_r. Constant contours of T_{wb} and ρ for $\alpha = 10$ are shown in Fig. 6. Using these coordinates improves decoupling between the directions corresponding to CF and both IFS and OFS. In reheat mode, the CF direction is well aligned with T_{wb}, but has little affect on ρ, while both IFS and OFS are well aligned with ρ, but have little affect upon T_{wb}. In cooling mode, the CF direction is well aligned with ρ. More importantly, using $(\Delta T_{wb}, \rho)$ instead of $(\Delta T_r, \Delta \phi_r)$ allows the fan speeds to be used to prevent overcooling at high $\Delta \phi_r$. In this region, the use of T_{wb} allows operation for small amounts of overcooling, where $\Delta T_r < 0$ but $\Delta T_{wb} > 0$.

Thus, in reheat mode, the fan speeds IFS and OFS control ρ, by closing a feedback loop with integral action to drive $\rho \rightarrow 0$. This feedback loop will effectively reduce the fan speeds when $\rho < 0$, avoiding the overcooled but high humidity region. The fans are coordinated in a prioritized manner, so that the IFS is actuated first, but if it reaches its minimum constraint, then the OFS is used, where it is effective. This can be achieved with the feedback controller diagrammed in Fig. 7, which employs a conventional anti-windup scheme. Also in reheat mode, CF regulates ΔT_{wb} instead of ΔT, slightly modifying the controller in Fig. 4, because it is better aligned with the CF direction. This strategy uses the fan speeds IFS and OFS to steer the trajectory along $\rho = 0$, and the CF to drive the trajectory through the origin in $(\Delta T, \Delta \phi)$ coordinates, so that both ΔT and $\Delta \phi$ are driven to zero simultaneously.

Cooling mode is used if $\rho > 0$ to drive the system to the $\rho = 0$ locus, and the switch between cooling and reheat modes occurs when $\rho = 0$. However, T_r is used as the feedback variable in cooling mode as in Fig. 4 to maintain consistency with conventional cooling-only equipment. With some hysteresis, this defines the simple, reliable and robust switching logic diagrammed in Fig. 8. Cooling mode is
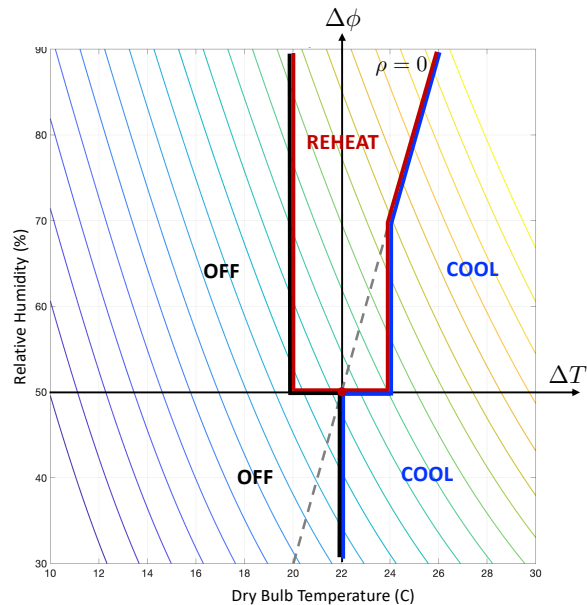
used when $\rho > 0$, except for the triangular region near the origin, which enlarges the reheat zone, and which is included to reduce undesirable switching between reheat and cooling modes. This strategy defines the feedback control architecture, and gains are tuned using conventional methods such as loop shaping or relay feedback using the Modelica model. Stability was checked and robustness margins were computed for a wide range of conditions.

V. SIMULATION RESULTS

Two simulation results are presented in this section. Figs. 9-10 show the result of a simulation with the multi-mode heat pump model connected to an adiabatic room model with a constant sensible heat disturbance $Q_s = 1.5$kW, a constant latent heat $Q_l = 1$kW, and initial air temperature of $35°$C at 70% relative humidity. The desired set point was $22°$C at 50% relative humidity. The system started in cooling mode, and the PI compensator drove the compressor speed to its maximum limit within a few minutes. The indoor air temperature was driven down while the relative humidity increased, as $\rho \rightarrow 0$. When $\rho = 0$, the system switched to reheat mode. Note that immediately after the switch, the evaporator temperature dropped approximately $8°$C, for reasons described in Section II, which increased the system latent heat capacity. Both indoor air temperature and humidity were driven to their set points simultaneously at 3.3h. Note that the indoor fan speed was modulated by the fan speed controller to its minimum limit, at which time the outdoor fan speed was modulated, to maintain $\rho \approx 0$ during the transient. Fig. 10 shows the transient in $(\Delta T, \Delta \phi)$ coordinates. This makes clear how cooling mode drove the system to the $\rho = 0$ locus, at which point reheat mode was engaged. In reheat mode, the coordinated fan speed controller
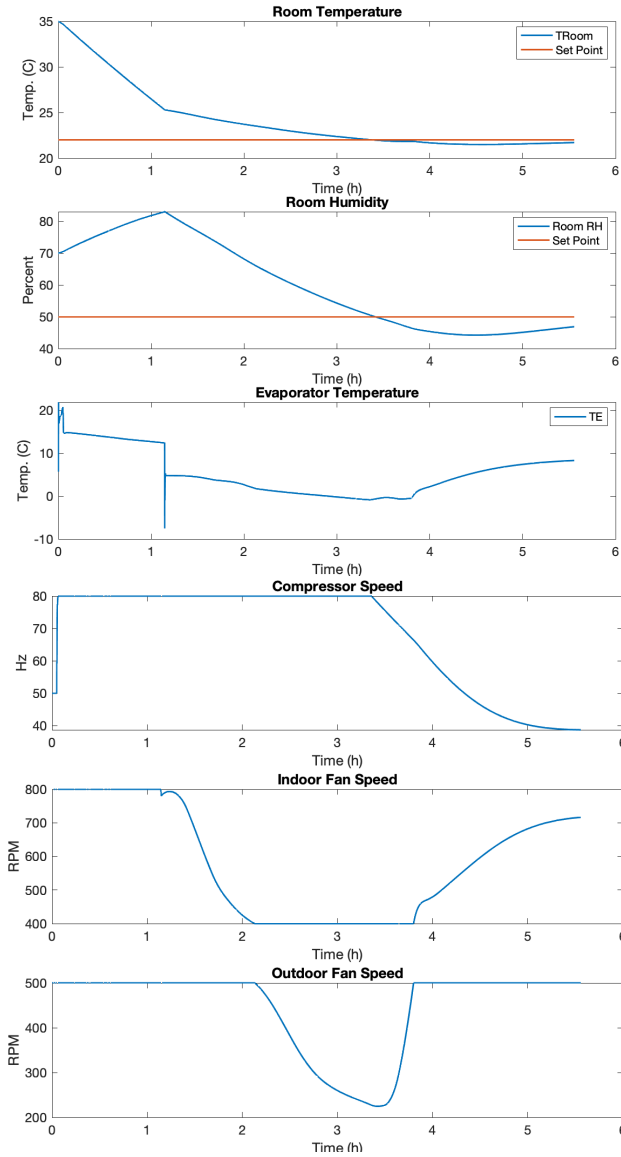
Fig. 9. Simulation of the multi-mode heat pump with an adiabatic room model with constant $Q_S = 1500W$ and $Q_L = 1000W$, showing T_r (top), T_e (second), CF (third), IFS (fourth) and OFS (bottom). Note the T_e transient during mode transition was caused by the start-up sequence, when the evaporator was almost starved of refrigerant, causing T_e to go below $0°C$ briefly, which is a genuine risk for this system architecture.

maintained $\rho \approx 0$ while the compressor controller drove the system through the origin.

The second simulation repeated the conditions shown in Fig. 1, but with the multi-mode heat pump. In this simulation, the automatic logic for transitions among cooling, reheat and off were fully defined using Modelica's synchronous features [24] and the Modelica StateGraph library [25] to realize discrete-event start-up and shut-down sequences. The off state means that the compressor and fan speeds were all set to zero. This state was intermediate between cooling and reheat. The simulation shows the effectiveness of the reheat mode in regulating indoor humidity, maintaining it
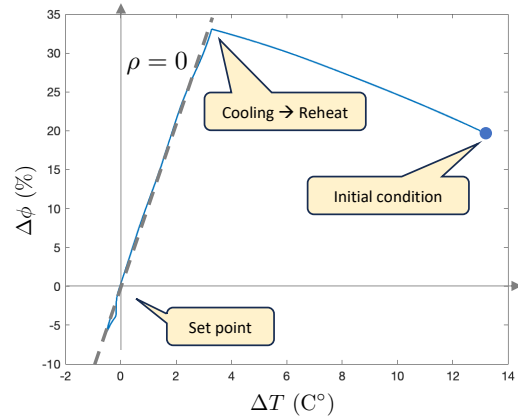

Fig. 10. Transient response of simulation in Fig. 9 in $(\Delta T, \Delta \phi)$ coordinates.

below 55%. The indoor and outdoor fan speeds were used to maintain $\rho \approx 0$, but in some extreme conditions during the second night, both fans saturated at their minimum values, so the ρ feedback loop opened. In these conditions it was not possible to regulate both T_r and ϕ_r to their set points with zero error, but the error is sufficiently small and in fact the machine was operating at its limits as best as possible.

VI. CONCLUSIONS

Replacing fossil fuel burning HVAC equipment with electric heat pumps is one of the most effective strategies to address global warming, but innovation is needed to develop products that operate in a wider range of conditions and climates. In this paper we considered a multi-mode heat pump that is capable of operating effectively in humid climate zones by regulating both indoor temperature and humidity. We used a hybrid system-level dynamic model of the multi-mode heat pump realized in the Modelica modeling language to derive, realize and simulate a simple but effective control strategy. The control algorithm includes an inner loop for regulating compressor frequency and expansion valves, an outer loop for controlling fan speeds, and hybrid logic to switch among a conventional cooling mode, a reheat mode, and an off state. The inner loop is largely conventional, while the fan speed control and mode switching logic is novel. The result was enabled by the use of object-oriented modeling and simulation, which capture the hybrid dynamics of the equipment and its coupling to building thermofluid dynamics.

REFERENCES

[1] B. Liu, M. Rosenberg, and R. Athalye, "National impact of ANSI/ASHRAE/IES standard 90.1-2016," in *2018 Building Performance Conference and SimBuild*. ASHRAE and IBPSA-USA, September 2018.

[2] M. Schulz, T. Kemmler, J. Kumm, K. Hufendiek, and B. Thomas, "A more realistic heat pump control approach by application of an integrated two-part control," *Energies*, June 2020.

[3] Y.-J. Kim, L. K. Norford, and J. James L. Kirtley, "Modeling and analysis of a variable speed heat pump for frequency regulation through direct load control," *IEEE Transactions on Power Systems*, vol. 30, no. 1, pp. 397–408, 2015.

[4] S. A. Bortoff, B. Eisenhower, V. Adetola, and Z. O'Neill, *The Impact of Automatic Control Research on Industrial Innovation: Enabling a Sustainable Future*. Wiley, 2024, ch. Building Automation.

[5] J. Winkler, J. Munk, and J. Woods, "Effect of occupant behavior and air-conditioner controls on humidity in typical and high-efficiency homes," *Energy & Buildings*, vol. 165, pp. 364–378, 2018.

[6] X. Xu, Z. Zhong, S. Deng, and X. Zhang, "A review on temperature and humidity control methods focusing on air-conditioning equipment and control algorithms applied in small-to-medium-sized buildings," *Energy & Buildings*, vol. 162, pp. 163–176, 2017.

[7] C. Younes, C. A. Shdid, and G. Bitsuamlak, "Air infiltration through building envelopes: A review," *Journal of Building Physics*, vol. 35, no. 3, pp. 267–302, 2011.

[8] M. Khattar, M. Swami, and N. Ramanan, "Another aspect of duty cycling: Effects on indoor humidity," *ASHRAE Transactions*, vol. 93, pp. 1678–1687, 1987.

[9] M. Wetter, W. Zuo, T. S. Nouidui, and X. Pang, "Modelica buildings library," *Journal of Building Performance Simulation*, vol. 7, no. 4, pp. 253–270, 2014.

[10] S. Zhan, A. Chakrabarty, C. Laughman, and A. Chong, "A virtual testbed for robust and reproducible calibration of building energy simulation models," in *18th IBPSA International Conference and Exhibition Building Simulation*, Sept. 2023.

[11] [Online]. Available: http://www.modelica.org

[12] *Modelica Language Specification Version 3.5*, Modelica Association, https://www.Modelica.org/, Feb. 2021.

[13] M. Otter, "Modelica overview," August 2011.

[14] K. I. Krakow, S. Lin, and Z.-S. Zeng, "Temperature and humidity control during cooling and dehumidifying by compressor and evaporator fan speed variation," *ASHRAE Transactions: Research*, vol. 101, no. 1, pp. 292–304, 1995.

[15] M. A. Andrade, C. W. Bullard, S. Hancock, and M. Lubliner, "Modulating blower and compressor capacities for efficient comfort control," *ASHRAE Transactions*, vol. 108, no. 1, pp. 631–637, 2002.

[16] X. Xu, S. Deng, and M. Chan, "A new control algorithm for direct expansion air conditioning systems for improved indoor humidity control and energy efficiency," *Energy Conversion and Management*, vol. 49, pp. 578–586, 2008.

[17] X. Han, X. Zhang, L. Wang, and R. Niu, "A novel system for the isothermal dehumidification in a room air-conditioner," *Energy & Buildings*, vol. 57, pp. 14–19, 2013.

[18] H. Fan, S. Shao, and C. Tian, "Performance investigation on a multi-unit heat pump for simultaneous temperature and humidity control," *Applied Energy*, vol. 113, pp. 883–890, 2013.

[19] P. Fritzon, *Principles of Object Oriented Modeling and Simulation with Modelica 3.3: A Cyber-Physical Approach*. Wiley, 2015.

[20] H. Qiao, V. Aute, and R. Radermacher, "Transient modeling of a flash tank vapor injection heat pump system–Part I: Model development," *International Journal of Refrigeration*, vol. 49, pp. 169–182, 2015.

[21] H. Qiao, C. R. Laughman, S. A. Bortoff, and D. J. Burns, "Dynamic characteristics of an R410A multi-split variable refrigerant flow air conditioning system," in *Proceedings of the 12th IEA Heat Pump Conference*, 2017.

[22] D. J. Burns, C. R. Laughman, and S. Bortoff, "System and method for controlling vapor compression systems," US Patent 10,495,364, Dec. 3 2019.

[23] S. Skogestad and I. Postlethwaite, *Multivariable Feedback Control: Analysis and Design*. Wiley, 2005.

[24] H. Elmqvist, M. Otter, and S. E. Mattsson, "Fundamentals of synchronous control in Modelica," in *Proceedings of the 11th International Modelica Conference*, 2011, pp. 15–25.

[25] H. Elmqvist, S. E. Matteson, and M. Otter, "Object-oriented and hybrid modeling in Modelica," *Journal Europeen des systems automatises (JESA)*, vol. 35, no. 1, 2001.
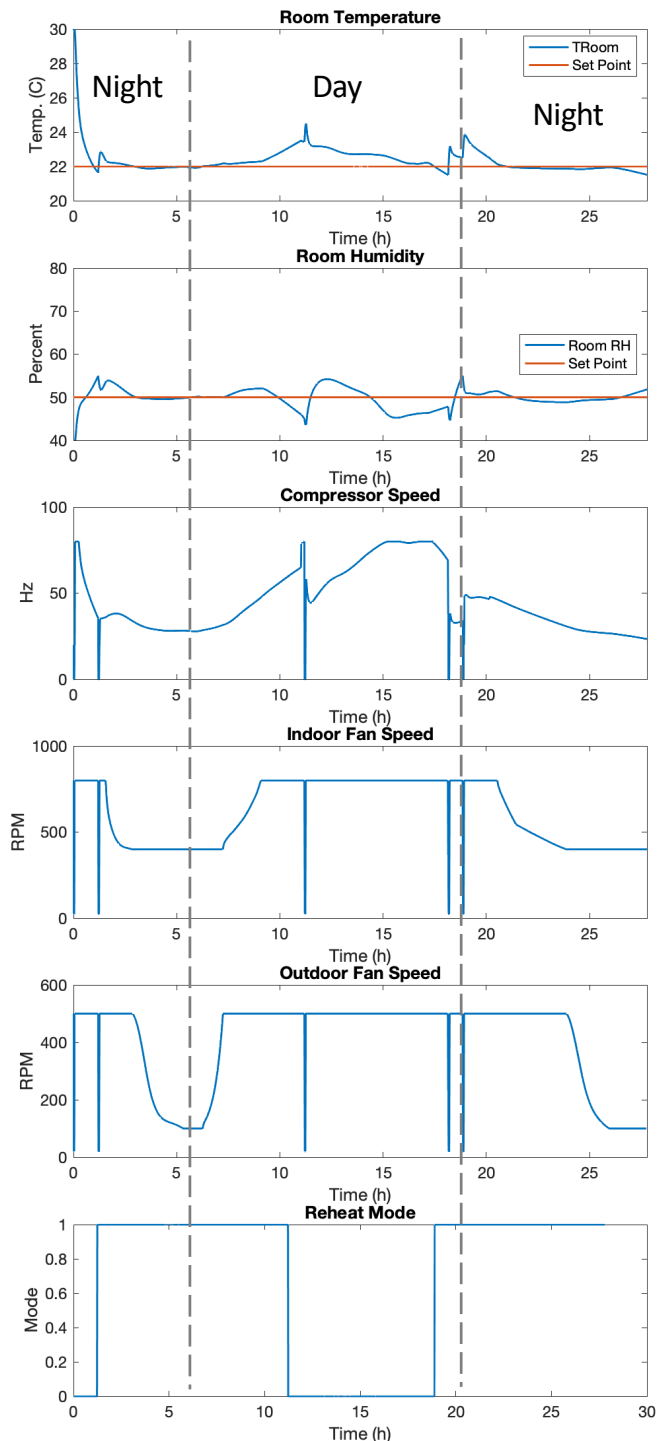
Fig. 11. Repeat of the simulation conditions in Fig. 1, but with the multi-mode heat pump and proposed control. Note the absence of on-off cycling, and the coordinated fan speeds.